# Hysteresis in the production of force by larval Dipteran muscle

Bethany A. Paterson[1], Ilya Marko Anikin[2] and Jacob L. Krans[2],*

[1]Department of Biological Science, Mount Holyoke College, South Hadley, MA 01075, USA and [2]Department of Biology, Central Connecticut State University, New Britain, CT 06050, USA

*Author for correspondence (kransjal@mail.ccsu.edu)

## SUMMARY

**We describe neuromuscular hysteresis – the dependence of muscle force on recent motoneuron activity – in the body wall muscles of larval *Sarcophaga bullata* and *Drosophila melanogaster*. In semi-intact preparations, isometric force produced by a train of nerve impulses at a constant rate was significantly less than that produced by the same train of stimuli with a brief (200 ms) high-frequency burst of impulses interspersed. Elevated force did not decay back to predicted values after the burst but instead remained high throughout the duration of the stimulus train. The increased force was not due to a change in excitatory junction potentials (EJPs); EJP voltage and time course before and after the high-frequency burst were not statistically different. Single muscle and semi-intact preparations exhibited hysteresis similarly, suggesting that connective tissues of the origin or insertion are not crucial to the mechanism of hysteresis. Hysteresis was greatest at low motoneuron rates – yielding a ~100% increase over predicted values based on constant-rate stimulation alone – and decreased as impulse rate increased. We modulated motoneuron frequency rhythmically across rates and cycle periods similar to those observed during kinematic analysis of larval crawling. Positive force hysteresis was also evident within these more physiological activation parameters.**

Key words: hysteresis, isometric force, *Drosophila*, *Sarcophaga*, muscle plasticity, kinematics.

## INTRODUCTION

The adaptability of an organism's repertoire of behaviors has important implications to the survival and evolution of that species. The synapse between nerve and muscle has long been utilized as a model of synaptic transmission and plasticity (Eccles et al., 1941; Keshishian et al., 1996), advancing our knowledge of the physiology of adaptability. The nerve–muscle preparation offers several exploitable attributes. Typically, muscle cells are accessible and simple to record from, they are large with basic geometry and they share several electrical properties with neurons. Investigations of neuromuscular transduction using model organisms, very many of which are either insects or crustaceans, have been particularly instructive of fundamental principles [e.g. larval fly (Griffith and Budnik, 2006); locust (Nivens and Burrows, 2003); crayfish (Pan and Zucker, 2009); crab (Nadim et al., 1999); and lobster (Marder and Bucher, 2007)].

Means of plasticity within the central nervous system has been the focus of much research but less is known about peripheral, muscle plasticity. Longer term (i.e. hours) structural plasticity of muscles has been described (Griffith and Budnik, 2006; Pette and Vrbová, 1999) but more rapid changes (i.e. seconds to minutes) such as mulluscan catch tension (Blaschko et al., 1931) remain relatively poorly understood. The dynamics of muscle cells are an important problem that continues to be investigated by several groups (Abbott and Aubert, 1952; Lappin et al., 2006; Dorfmann et al., 2008; Woods et al., 2008; Zill et al., 1992). Advances in our understanding of non-linearities and plastic elements of muscle provide insight to the control and modulation of motor behavior. One example of post-synaptic muscle plasticity that is unique to the periphery is neuromuscular hysteresis. Neuromuscular hysteresis encompasses several historical phenomena, such as the 'Blaschko effect' (Blaschko et al., 1931) and catch tension (Wilson and Larimer, 1968; Zill and Jepson-Innes, 1988), and is generally the deviation in force

production from a predictive motoneuron rate– (or strain–) force curve because of recent activity at the neuromuscular junction or muscle itself. Specifically, forces generated by a constant-rate train of motoneuron potentials differ greatly from those obtained from the same train with a transient (i.e. <<1s) change in motoneuron rate interspersed, and are not the result of modified muscle depolarization (e.g. facilitation or depression). Furthermore, some work has suggested the increased force cannot be explained by maintained increases in intramuscular calcium (Hoyle, 1983).

We describe hysteresis in force production by larval fly muscle that arises with brief but robust changes in motoneuron activity (e.g. Krans and Chapple, 2005; Wilson et al., 1970). Although force hysteresis is brought about by transient changes in motoneuron rate or muscle strain, the change in force is longer lasting (Abbott and Aubert, 1952; Harrison et al., 2008; Krans and Chapple, 2005; Wilson and Larimer, 1968). Hysteretic force can differ by an order of magnitude from predicted force values, and may be either positive or negative in sign, depending upon the addition or omission of nerve impulses, respectively (Burke et al., 1970; Wilson and Larimer, 1968). Positive hysteresis is evident in a diverse collection of organisms inclusive of both vertebrate and invertebrate clades, suggestive of the phenomenon's generality [Chordata (Burke et al., 1970; Harrison et al., 2008; Avrova et al., 2009); Mullusca (Andruchov et al., 2006); Arthropoda Insecta (Blaschko et al., 1931; Zill and Jepson-Innes, 1988; Zill et al., 1992; Dorfmann et al., 2008); Arthropoda Crustacea (Wilson et al., 1970)].

Muscle plasticity presents a problem to the motor control system in that deviations from predictive rate–force relationships make accurate or precise recruitment of force a more dynamic task. Hypothetically, such variability of force output could be overcome with feedback sensors able to indicate gain in the rate–force relationship between nerve and muscle. However, to our knowledge, no such afferent feedback mechanism has been

described. Although several afferents are able to modify muscle gain, for example, vertebrate muscle spindles (Hunt, 1990) or those of the visual system (Donaldson and Knox, 2000), there does not appear to be evidence that the signal being transmitted is gain itself. Zill and Jepson-Innes proposed that muscle hysteresis (i.e. catch tension) may be compensatory for the negative hysteresis exhibited in afferent coding/firing (Zill and Jepson-Innes, 1988). Non-linearities of the input system could be well matched with those of the output system such that they accommodate one another yielding a pseudo-linear system. This is an enticing hypothesis for which there are some supporting data but too few afferent systems and preparations are adequately understood to adopt it as a general explanation for the problem of hysteresis in neuromuscular control. Here, we report on the parameters of hysteresis in body wall muscles of larval *Diptera*, which we feel can be especially useful preparations in the effort to elucidate the relationship between neural control and muscle plasticity. They offer easily accessible and robust muscle cells that are innervated by a well-documented system of segmental nerves (Keshishian et al., 1996). Quantitative data are easily acquired from these preparations, making them useful for probing the parameters of the neuromuscular transform. The motor behavior of larvae is also well documented (Barrigan and Pepin, 1995; Fox et al., 2006), allowing the placement of quantitative results into a behavioral context.

In much of the historical literature describing hysteretic effects, there is a putative behavioral role for hysteresis. For example, in Mullusca and Crustacea, positive hysteresis may provide some level of energy conservation (Twarog, 1972; Wilson and Larimer, 1968). During sustained contractions, fewer motoneuron action potentials are required to maintain a particular tone post-transient activation (Krans and Chapple, 2005; Twarog, 1972). Fly larvae are particularly interesting because their repetitive rhythmic contractions do not offer a compelling behavioral value of hysteresis. What is the benefit to larvae, which engage in a relatively simple motor behavior of undulatory contraction, of dynamic modification of the rate–force relationship? We propose that the presence of hysteresis in fly larvae supports the generality of this form of muscle plasticity.

## MATERIALS AND METHODS
### Animals
*Sarcophaga bullata* Parker were purchased from Carolina Biological Supply (#144440, Burlington, NC, Canada). Larvae were placed in two-quart containers with a custom food recipe consisting of woodchips, yeast, sugar, dried milk, Tegasept (mold inhibitor, #H6654, Sigma-Aldrich, Allentown, PA, USA) and raw beef liver. Animals were maintained at 20°C in an incubator on a 12 h:12 h light:dark cycle until they tanned. Newly eclosed adult flies were moved to rearing containers with scored liver at 23°C. Upon appearance of larvae, adults were removed and the containers were placed back into containers at 20°C. This temperature routine extended the duration of larval instars and thus the time available for experimentation. Only wandering stage third instar larvae were selected for experiments.

Wild-type *Drosophila melanogaster* Meigen (Canton-S, CS-5 stock) were raised at 20°C in vials on standard diet (from David, 1962), consisting of: 100 g yeast; 100 g glucose; 12 g agar; 10 ml propionic acid (mold inhibitor), combined in 1220 ml $H_2O$. As with *Sarcophaga* larvae, only wandering third instar larvae were selected for physiological experiments; no animals exhibiting trachea eversion, tanning or reduced locomotion were selected.

### Physiology
Experiments utilizing *Sarcophaga* were performed in insect saline (Strausfeld et al., 1983) composed of (mmol l$^{-1}$): Na$^+$ 144; Cl$^-$ 161; Ca$^{2+}$ 7; K$^+$ 5; Mg$^{2+}$ 1; HCO$_3^-$ 4; TES 5; trehalose 5; sucrose 100; pH 7.1. *Drosophila* experiments were performed in HL-3, described in detail by Stewart et al. (Stewart et al., 1994). Temperature was maintained during *Sarcophaga* experiments between 16°C and 18°C *via* recirculation of coolant through the preparation stage. *Drosophila* data were obtained at 20–23°C (room temperature) as we noticed a substantial reduction in contractibility at lower temperatures.

Muscle force was recorded using a custom force transducer composed of four silicon wafer strain gauges (Micron Instruments, Simi Valley, CA, USA) in full Wheatstone bridge configuration (Allen et al., 1980). The larval body wall was attached directly to the beam of the transducer rather than a lever arm or secondary beam. The force transducer operated with a gauge factor of ~400. No signal amplifier or filtering was required for *Sarcophaga* force data; gain of the data acquisition board was set to one. A differential amplifier was used during *D. melanogaster* recordings (model 3000, A-M Systems, Carlsborg, WA, USA) but no online filtering was needed. The transducer operated linearly between 0.01 mN and 2 N (calibrated using aluminium foil fragments of known mass, $R^2$=0.99) and exhibited no temperature sensitivity between 10°C and 30°C. Contractions were approximately isometric; whole animal contractions (~1 N) flexed the transducer less than 500 µm and single muscle contractions produced no visible deformation of the transducer beam.

Three preparations were used for force recordings: (1) intact animals, (2) semi-intact animals, and (3) single nerve–muscle preparations. In all cases, Plexiglas tabs containing stainless steel hooks (Fig. 1) were glued to the larval cuticle so that (a) one end could be securely fastened to the substrate, and (b) one end could be attached to the force transducer (Fig. 1B,C).

### Intact larvae
We used an HD camcorder (model 595V, DXG USA, City of Industry, CA, USA) to record video for 10–20 s of wandering phase locomotion shortly after larvae were removed from the rearing containers. Videos were parsed into five still frames per second using QuickTime Pro (Apple, Cupertino, CA, USA). Body length, width and anterior direction were measured per frame using ImageJ (NIH, Bethesda, MD, USA). Also, force generation during larval crawling was recorded from intact animals with their posteriors attached to the beam of the force transducer; they were otherwise free to ambulate (in place). Forces were recorded as the animal attempted to crawl toward a bright light. These experiments provided an estimate of the rate of undulatory locomotion, which was used in later nerve stimulus paradigms. Isometric forces from the longitudinal body wall musculature were recorded from the second and third preparation types, i.e. semi-intact preparations and single nerve–muscle cell preparations.

### Semi-intact larvae
Dissections of *Sarcophaga* were performed as described by Feeney et al. (Feeney et al., 1998). During dissection, larvae were pinned (size 00; VWR International, West Chester, PA, USA) at their posterior and anterior apexes to a Sylgard-lined dish (Dow Corning Corporation, Midland, MI, USA). A shallow longitudinal incision was made from posterior to anterior along the dorsal midline. Guts and tracheae were removed to expose the body wall musculature and segmental nerves. Segmental nerves were severed where they exited the ventral ganglion and gathered into a suction electrode if
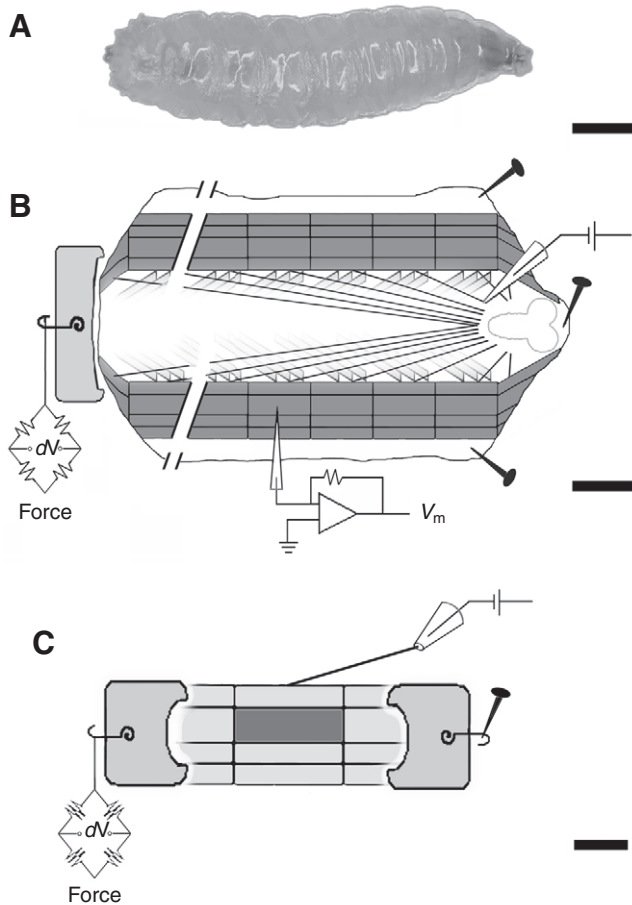
Fig. 1. Preparations used for force recordings and physiology. (A) Whole animal preparation. A micrograph of a third instar *Sarcophaga bullata* larva is shown, scale bar=2 mm. (B) Semi-intact preparation. A schematic of a filleted larva highlights the longitudinal muscles (M6, M7, M12 and M13), which produced the gross majority of longitudinal force discussed herein. Transverse muscles are indicated by fading light gray, outlined in the center of the schematic. Segmental nerves are shown as black lines radiating from the ventral ganglion (at right). Plexiglas tabs, stimulating and recording electrodes are shown. Scale bar=2 mm. (C) Single nerve–muscle preparation. Ablated muscles are shown as light gray whereas the chosen muscle for recordings is in dark gray. A single nerve is gathered into the stimulating electrode and tabs are attached as described in text. Scale bar=1 mm. $V_m$, membrane potential; $dV$, voltage difference.

stimulation was required (Fig. 1B). Dissections of *Drosophila* were performed similarly, and as described previously (Krans et al., 2005; Krans et al., 2010).

### Single cells

Dissections were carried out as described above for single nerve–muscle preparations, and additionally, all longitudinal muscles with the exception of one were manually ablated using fine forceps or vanos scissors (Fig. 1C). The force transducer was secured to the cuticle of the ablated muscle – again *via* a glued tab – directly posterior to the chosen muscle segment whereas the cuticle beneath ablated muscles, which were anterior to the chosen segment, were secured to the Sylgard with insect pins.

In all experiments, contractions generated by single motor nerve stimuli were monitored as muscle was stretched until reaching the approximate peak of the length–tension curve. This peak was identified empirically as the muscle length just shorter than that at

which a decrease in force occurred. This method ensured that data were obtained from muscles at comparable positions on the length–tension curve and that rate–force curves could be compared across animals of varied size.

Intracellular voltage recordings were made from the muscle of semi-intact preparations. Thin wall glass microcapillary tubes (1.0 mm IN, World Precision Instruments, Sarasota, FL, USA) were pulled by a Flaming/Brown Micropipette Puller (P-87 or P-97, Sutter Instrument Co., Novata, CA, USA) to resistances of ~40 MΩ. Microelectrodes were filled with $2\,\mathrm{mol\,l^{-1}}$ potassium acetate and were mounted to a micromanipulator (Narishige International USA, Inc., Long Island, NY, USA). Membrane potentials were measured using an AxoClamp-2A amplifier (Axon Instruments, Union City, CA, USA).

Severed segmental nerves were gathered into and stimulated using glass suction electrodes. Tips were fire polished to the desired luminal opening for nerve suction. Stimulus current was modulated by a Grass S88 stimulator (Grass Instruments, West Warwick, RI, USA) and isolated from recordings *via* an isolation unit (SIU5, Grass Instruments). Stimulus threshold of the motoneuron was established using two values: (1) the minimum stimulus magnitude required for a single, compound junction potential observed *via* intracellular recording, and (2) the stimulus magnitude that consistently recruited muscle contractions. Final stimulus magnitude was set between 125% and 150% of these thresholds. Trials were displayed on an oscilloscope (Tektronix, Beaverton, OR, USA) and recorded *via* an I/O, A-D board (6024E, National Instruments, Austin, TX, USA) using custom routines composed using the MATLAB DAQ toolbox (MathWorks, Natick, MA, USA).

Three different experimental stimulus paradigms were used: (1) constant-rate, (2) hysteretic burst, and (3) frequency-modulated stimulation. Constant-rate stimulation (1) involved a simple train of stimuli at a constant frequency. Hysteretic stimulation (2) used the same trains as in the constant-rate paradigm but interspersed a 200 ms burst (50 Hz) midway through the trial. During constant-rate and hysteretic stimulus trains, the constant-rate portion of stimulation was selected randomly from the following frequencies (Hz): 2, 5, 7, 10, 12, 15, 20, 30 and 40. Frequency-modulated stimulation (3) utilized sinusoidal stimulus frequency modulation. Timing was controlled using custom DAQ routines. Coding specific inter-stimulus intervals into set cycle periods was not trivial because the range of frequencies could be limited by short cycle periods. Cycle frequency was increased sequentially in 1 Hz steps from 2 Hz to 25 Hz and then decreased sequentially back to 2 Hz (total burst duration=5.6 s) or increased and then decreased sequentially over the same range in 0.5 Hz steps (total duration=10.6 s). For example, the period required to present a 2 Hz, 3 Hz, 4 Hz... 25 Hz, 24 Hz, 23 Hz.… 4 Hz, 3 Hz, 2 Hz cycle can be computed as the sum of all intervals (s): $\Sigma(t)^{2-25-2\mathrm{Hz}}=(0.5+0.33+0.25+\ldots+0.04+\ldots+0.25+0.33+0.5)=5.59\,\mathrm{s}$.

Lastly, stimulus artifacts were attenuated in single trial force plots, but not averaged traces, by using a low-pass filter with a cut-off of 5 kHz.

Force was measured as the change from resting tonus to the plateau phase of a given contraction. The first and last stimulus train for all experiments was a single, 3 s, 50 Hz constant-rate burst. The forces produced by the first and last 50 Hz constant-rate bursts were averaged because force production tended to decrease slightly over a 40–50 min experiment. In order to normalize force to each muscle's maximal production (i.e. 50 Hz stimulation) over the whole experiment, the mean of initial and final constant-rate values were used.

## Data analysis

Experiments consisted of four to six 'sets' of a particular stimulus paradigm and rate. Each set ranged from five to 10 repetitions, with intertrial pauses of 45 s for constant-rate, 65 s for hysteretic and 75 s for frequency-modulated paradigms. This yielded between 20 and 60 repetitions for each experimental condition. The number of biological replicates ($N$) is given as the number of animals, not repetitions. Standard error of the mean is computed using the number of animals and is reported unless otherwise noted. Fit equations, correlation values and $t$-test probabilities were generated using the statistics toolbox in MATLAB (Mathworks). Sigmaplot (Systat Software, San Jose, CA, USA) was used to generate basic hyperbolic fits (single rectangular, two parameters and intercept). Formulae are given in figure legends where possible.

Some data have been reported previously in abstract form (Paterson and Krans, 2009).

## RESULTS

We first quantified the isometric force generated by constant-rate trains of stimuli to the motoneuron(s) to generate a predictive rate–force relationship (Fig. 2). Individual stimuli evoked visible contractions from body wall muscle. Forces did not augment or facilitate but did summate as rate increased (Fig. 2A semi-intact,

and Fig. 2C single muscle). Generally, force increased with stimulus rate and saturated at ~20 Hz (Fig. 2B,D).

We overlaid averaged force traces from single muscle and semi-intact preparations ($N$=5, each trace; Fig. 2E) to compare time constants of contraction. The time constants (time to reach ~63% of asymptotic force: $\tau_{rise}$) of force produced by semi-intact and single muscle preparations were not statistically different (0.54±0.016 s, 0.56±0.041, respectively, $P$<0.01). Similarly, latency to peak force using semi-intact animals was 1.26±0.038 s and 1.30±0.062 in single muscles ($P$<0.01). The ratio of single to semi-intact force magnitudes across all comparable stimulus rates was 1:55.15±3.84 ($N$=64 recordings). Because force generated by single muscles was necessarily less than semi-intact animals, the absolute values from Fig. 2B,D were normalized to the maximal force of the preparation from which data were obtained (Fig. 2F). The hyperbolic functions used here illustrate the relationship between rate and force, providing an estimate of the rates at which the preparations reach 50% and 90% maximal force. The two rate–force curves are similar: half-saturation occurred at 4.43 Hz for semi-intact animals and 4.90 Hz for single muscle preparations, and 90% saturation occurred at 19.47 Hz for semi-intact and 17.09 Hz for single muscle preparations.

We next evaluated the smaller muscle of *D. melanogaster*. The rate–force relationship of *Drosophila* was strikingly similar to that
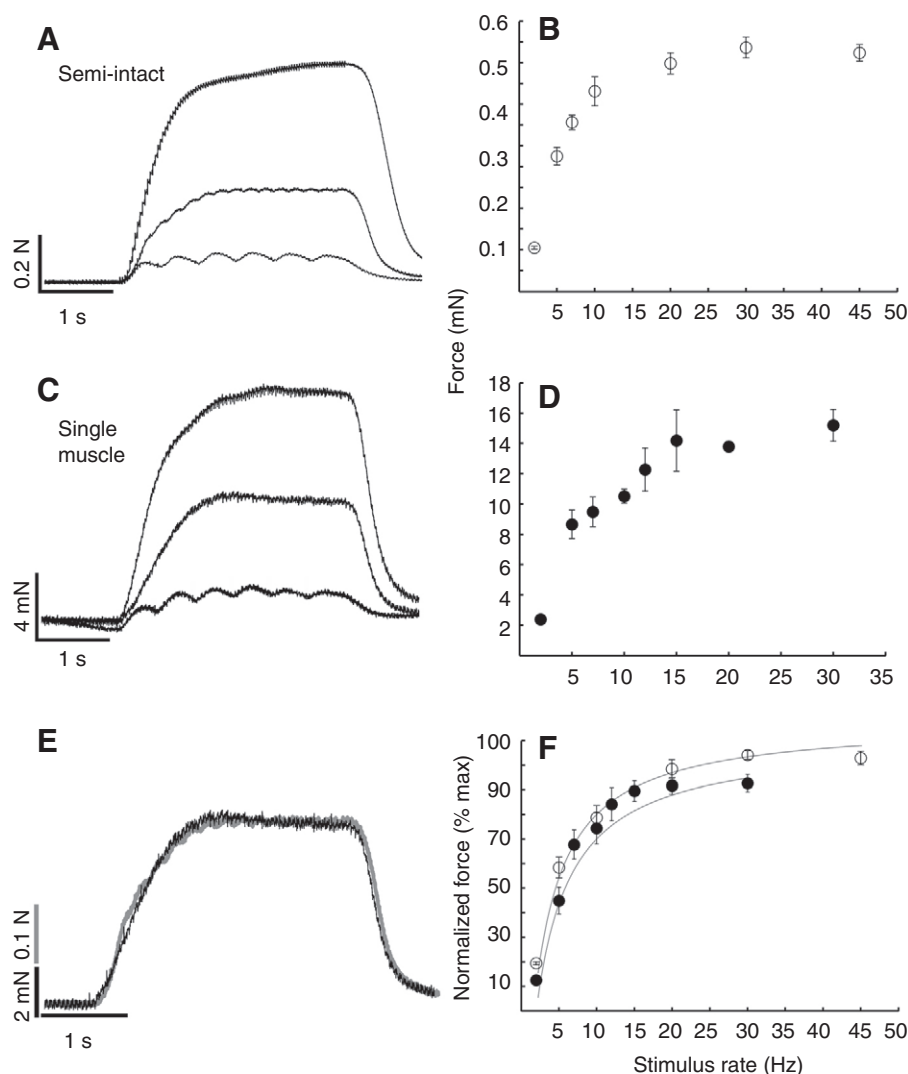


Fig. 2. Force generated by *Sarcophaga bullata* body wall muscle from constant-rate stimulus trains. (A) Force traces from the semi-intact preparation. Force generated by 4 s constant-rate stimulus trains to the segmental nerve at 2, 5 and 30 Hz are shown (bottom to top). Inflections indicate stimulus times. (B) Semi-intact motoneuron rate–muscle force relationship. Force increases monotonically with motoneuron rate and saturates at rates above ~20 Hz ($N$=32). (C) Force traces from single muscle preparations. Constant-rate stimulus trains as in panel A but at 2, 10 and 20 Hz. (D) Single muscle rate–force curve. As in semi-intact preparations, force produced by single muscles increases with stimulus rate and saturates ~20 Hz ($N$=32). (E) Overlay of semi-intact (gray) and single muscle (black) force records from 5 Hz stimulation. (F) Normalized force–rate curves. Data from panels B and D are normalized to peak force obtained from each animal, as described in the Materials and methods. Hyperbolic functions illustrate the similarity between stimulus rates at which half-maximal and 90% force is generated {open circles: semi-intact, force=−0.55+[(1.70×rate)/(2.55+rate)], $R^2$=0.99; 50% force=4.44 Hz, 90% force=19.47 Hz; closed circles: single muscles, force=−0.58+[(1.66×rate)/(2.86+rate)], $R^2$=0.99; 50% force=4.90 Hz, 90% force=17.09 Hz}.

of *Sarcophaga* despite their different biology, increased variability and the reduced signal to noise ratio of data obtained from the smaller muscle (Fig. 3A). Force increased monotonically with stimulus rate in *Drosophila* semi-intact preparations as it did in *Sarcophaga*. We once again used a hyperbolic function to estimate the rates at which 50% and 90% force saturation occurred (8.73 Hz and 29.90 Hz, respectively; Fig. 3B).

Having established rate–force relationships using a constant-rate stimulus paradigm, we proceeded to investigate deviations from these relationships upon introduction of a brief (200 ms), high-frequency (50 Hz) burst of motoneuron potentials – a 'hysteretic burst' – midway through an otherwise constant-rate train of stimuli (*Sarcophaga*, Fig. 4; *Drosophila*, Fig. 5). In addition to a transient increase in force concurrent with the hysteretic burst of stimuli, force remained elevated for the duration of stimulation (Fig. 4A, semi-intact; Fig. 4B, single muscle). The second half of each paradigm's stimulus train was composed of identically timed stimuli but force generated after the hysteretic burst failed to decay back to predicted constant-rate values. Rather, force approached a constant value much greater than that predicted by constant-rate stimulus alone. To quantify the force produced by a hysteretic stimulus paradigm, force values at the termination of stimuli were compared with those of constant-rate stimulation. Both semi-intact (Fig. 4A) and single muscle (Fig. 4B) preparations generated and sustained increased force after the brief high-frequency burst, a phenomenon hereafter termed 'positive hysteresis'.

The magnitude of positive hysteresis was greatest at low frequency and diminished as stimulus rates increased and the resultant force approached saturation (*Sarcophaga*, Fig. 4C–F; *Drosophila*, Fig. 5C,D). Positive hysteresis was significant among *Sarcophaga* larvae in trials wherein the constant-rate portions of stimulation were 2, 5 and 7 Hz ($P=0.011$, $P=0.048$ and $P=0.052$, respectively). At two stimuli per second, positive hysteresis yielded force that was $2.10\pm0.014$ times the predicted value based on constant-rate stimulation. The difference between hysteretic and constant-rate force values was quantified as:

$$\% \text{ increase} = \left\{ \frac{\left| F_{\text{hysteretic}} - F_{\text{constant-rate}} \right|}{F_{\text{constant-rate}}} \right\}. \qquad (1)$$

Thus, a $2.10x$ increase in force was recorded as ~110% increase over the force generated by constant-rate stimulation alone. Positive hysteresis decayed as stimulus rate increased (Fig. 4E,F). Exponential functions fit these data well ($R^2_{\text{semi-intact}}=0.89$, $R^2_{\text{single}}=0.91$), and the slopes for both single muscle and semi-intact preparations were similar (semi-intact, $e^{-0.162}$; single muscle, $e^{-0.186}$; Fig. 4).

Among *Drosophila* larvae, force generated by hysteretic stimulus paradigms was also greater than that generated by constant-rate stimulus paradigms (Fig. 5A,B) but the increase was significant only at the lowest reported stimulus frequency, 10 Hz ($P=0.048$), yielding a 68.6% increase in force (Fig. 5C). Similar to the larger larvae, positive hysteresis decayed as stimulus rate increased (Fig. 5D, exponential model $R^2=0.91$). Generally, the hysteretic force gains observed in *D. melanogaster* larvae were less dramatic than the larger *S. bullata*. The intercept of the exponential function used to fit force gain *via* hysteretic stimulation in *Drosophila* (Fig. 5D) was half that of the larger flies (*Drosophila*=49.8%, mean *Sarcophaga*=105.79%), and the slope of the relationship in fruit fly was similarly about half as steep ($e^{-0.087}$ and $e^{-0.174}$).

Our initial hypothesis was that increased force following a hysteretic burst was the result of EJP facilitation. We recorded EJPs during hysteretic stimulus paradigms and found no difference between the amplitude or rise time of EJPs before or after a hysteretic burst despite a marked increase in force (EJP$_{\text{pre-burst}}$=$24.54\pm1.32$ mV; EJP$_{\text{post-burst}}$=$23.84\pm0.97$ mV; $P<0.01$; Fig. 6A,B). Rise and fall rates of EJPs recorded before and after a hysteretic burst were not statistically different (pre-burst, $\tau_{\text{rise}}$=$6.91\pm0.41$ ms, $\tau_{\text{decay}}$=$94.23\pm1.31$ ms, $N=140$ EJPs; post-burst, $\tau_{\text{rise}}$=$7.51\pm0.19$ ms, $\tau_{\text{decay}}$=$89.70\pm1.28$ ms, $N=140$ EJPs; $P<0.05$, both). Moreover, EJPs recorded before or after a burst were not different from those recorded from a constant-rate stimulus train without a hysteretic burst (data not shown). We recorded EJPs across a series of stimulation frequencies to investigate if there was a rate at which the addition of a hysteretic burst gave rise to a difference in synaptic potentials. During the constant-rate portion of any given stimulus paradigm, the amplitude of successive EJPs was well conserved; no changes in synaptic voltage were noted from potential to potential (Fig. 6C). We found that as stimulation rate increased, and thus inter-EJP intervals decreased, EJP amplitude also decreased (Fig. 6D). EJP amplitudes before and after the hysteretic burst decayed similarly with increased stimulus frequency and were fit by the same linear equation.

It remained unclear if the lower rates at which hysteresis offers large gains in the rate–force relationship were relevant to the behaving animal, so we next recorded parameters of motor behavior observed from intact and semi-intact preparations. Intact, untethered larvae crawled toward a bright light with a contraction rate of about 0.83 Hz (period $1.14\pm0.26$ s; Fig. 7A), slightly slower than that described for the similar sized *Calliphoridae* larvae (Berrigan and Lighton, 1993). Upon tethering the intact animal's posterior end to our force transducer whilst leaving the anterior end free to pull, rhythmic contractions occurred more slowly, at a rate of ~0.17 Hz (period=$5.81\pm0.25$, $N=15$; Fig. 7B), similar to rates reported for *Drosophila* (Fox et
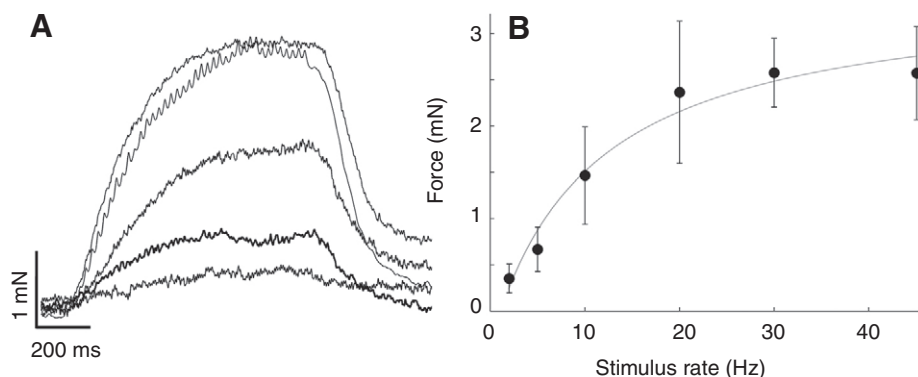


Fig. 3. Force generated by *Drosophila melanogaster* body wall muscle from constant-rate stimulus trains. (A) Force produced by the semi-intact larvae upon stimulation of the segmental nerves at 2, 5, 10, 20 and 30 Hz. (B) As in *Sarcophaga* muscle, force increases with stimulus rate monotonically and saturates between 20 Hz and 30 Hz {$N=6$ animals, force=$-0.37+[(3.85\times\text{rate})/(10.54+\text{rate})]$, $R^2=0.97$}.
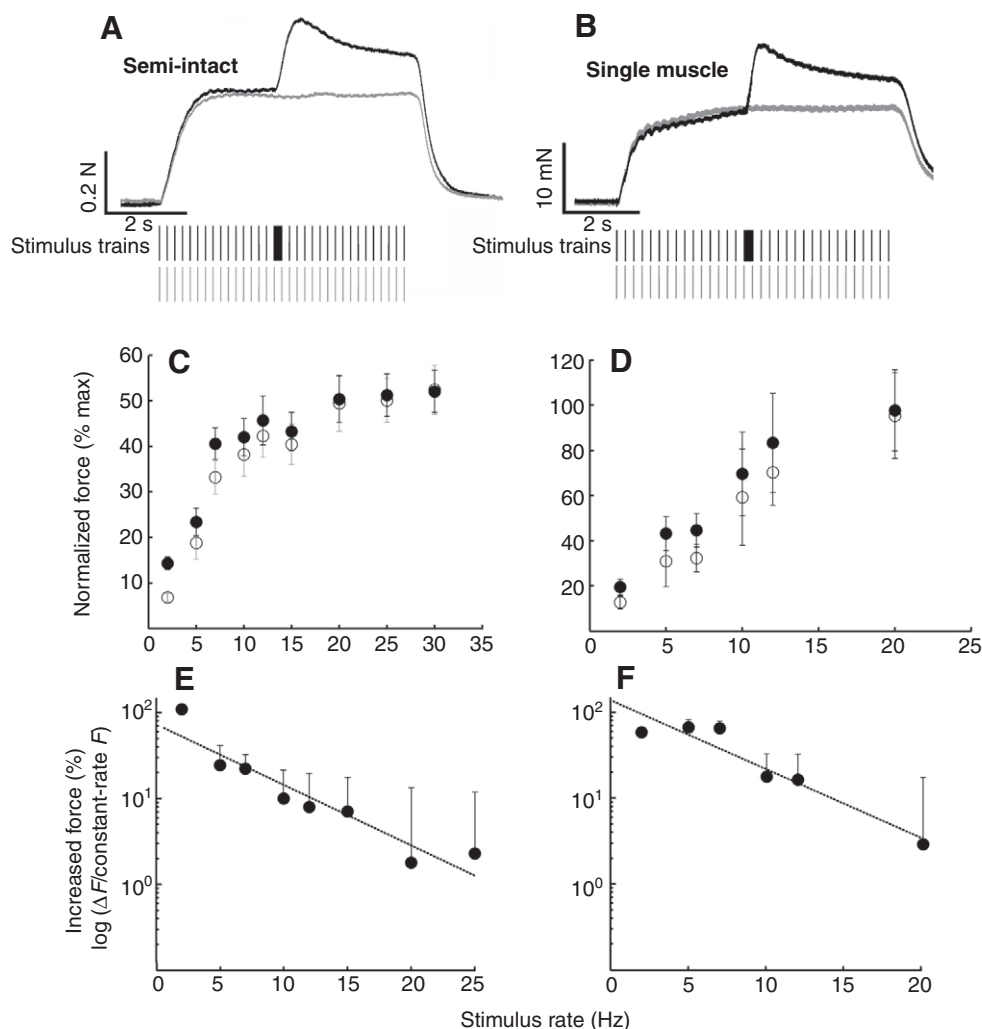
Fig. 4. Hysteretic force generation by larval body wall muscles of *Sarcophaga bullata*. Left column: data gathered from semi-intact preparations. Right column: data gathered from single nerve–muscle preparations. (A) Both constant-rate (10 Hz, gray) and hysteretic (black) stimulation records are shown. The hysteretic burst of stimuli to the segmental nerve (50 Hz, 200 ms) is indicated on the stimulus train plots (bottom) by the thick black bar at $t$=4 s. After the hysteretic pulse, stimulus trains are identical but hysteretic force remains much greater than constant-rate force. (B) Force traces and experimental design are as in panel A but data are from single nerve–muscle preparations. (C) Forces generated upon hysteretic stimulation (closed circles, $N$=65) represent the force value 1 s before the end of stimulation – the maintained rather than transient difference in force. Forces generated by a hysteretic stimulus paradigm exceed those of constant-rate stimulation (open circles, $N$=65), although the difference decreases as the constant-rate frequency increases and is fully attenuated by 20 Hz. (D) Similar to semi-intact results, the difference between single muscle hysteretic force (closed circles, $N$=28) and constant-rate (open circles, $N$=32) force decreases as stimulus rate increases. (E) Increased force generated by hysteretic *vs* constant-rate force is plotted as a function of stimulus rate. Difference in force is shown as a percentage [(hysteretic/constant-rate) $\times$100] and fit with an exponential equation (% increase=$72.98e^{-0.162(\text{rate})}$, $R^2$=0.89). As in E, (F) illustrates the increase in hysteretic force over a range of stimulus rates and fit with a notably similar exponential equation, % increase=$138.60e^{-0.186(\text{rate})}$. Only positive error bars are plotted.

al., 2006). Contractions of the tethered, intact animal regularly occurred at multiples of 5.5 s (i.e. 11 s, 16.5 s and 27.5 s; Fig. 7C). The underlying synaptic potentials of these contractions occurred in bursts with similar periods despite the reduction of the preparation from tethered intact to semi-intact (Fig. 7D, inset). The range of EJP rates that gave rise to these contractions varied rhythmically from burst to burst. A typical example of EJP rate during and after a single burst is shown in Fig. 7D. The inter-EJP interval and resultant instantaneous frequency ranged from about 0.04 s to 1.2 s and thus ~25 Hz to ~1 Hz (Fig. 7E).

We developed a custom stimulus routine to cyclically modulate rate of motoneuron activation to test whether hysteretic force gains persisted during more behavioral activation patterns. This stimulus paradigm allowed us to test EJP rates comparable with those

described above (Fig. 7) as well as modulate through frequencies and cycle periods observed of tethered, intact animal crawling.

Modulating stimuli between 2 Hz and 15 Hz over a cycle period of six seconds gave rise to rhythmic contractions similar in shape to those observed from the intact, tethered larvae (compare Fig. 8A and the final contraction of Fig. 7B). Specifically, each successive contraction was similarly asymmetrical such that the rising phase of force production appeared concave and the falling phase appeared convex. This profile clearly exhibits positive hysteresis; the force generated at 10 Hz along the falling phase of contraction, for example, was 142.7±9.53% ($N$=9 animals) greater than that generated by 10 Hz stimulation during the rising phase of contraction (Fig. 8A,B; arrows indicate phase). The magnitude of hysteresis is quantified here as the difference between force generated at a single
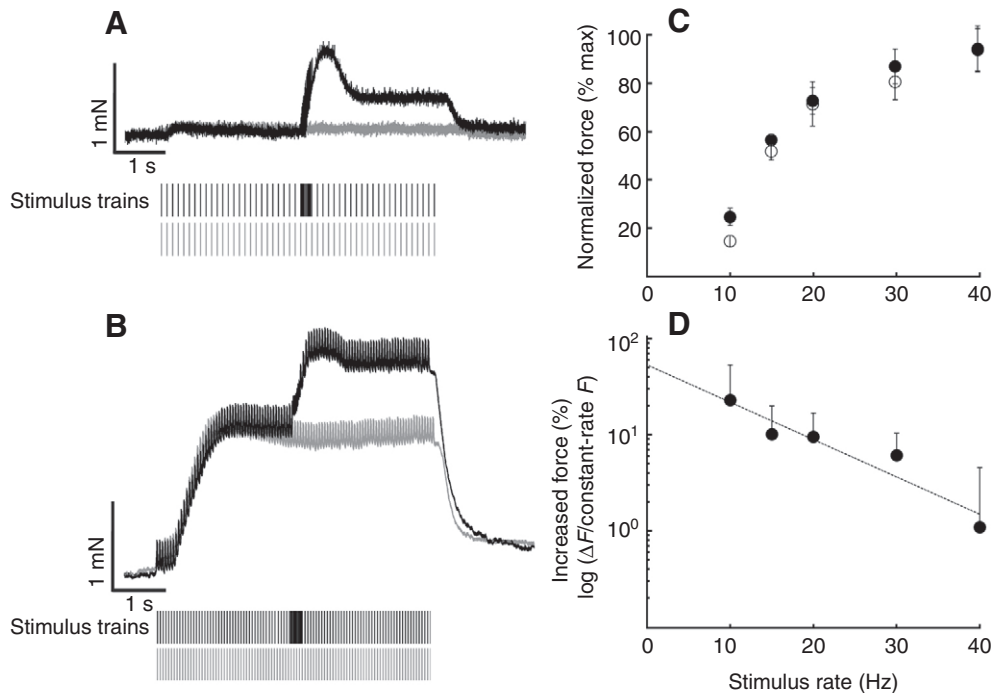
Fig. 5. Hysteretic force production by larval *Drosophila melanogaster* body wall muscle. (A) A single trial example of positive force hysteresis following a brief high-frequency stimulus burst to the segmental nerve (as before, 200 ms, 50 Hz). Force gains *via* the hysteretic paradigm (black) were most pronounced when the frequency of the constant-rate portions of the stimulus train were low, herein the constant-rate frequency was 10 Hz. (B) The mean of five trials of hysteretic stimuli (20 Hz constant-rate portions, 50 Hz, hysteretic burst). (C) Force was greater following a hysteretic stimulus paradigm (closed circles) than constant-rate stimulus alone (open circles, $N$=59). The increase in force was significant only when the constant-rate frequency was low (i.e. 10 Hz, $P$=0.048), and the difference between force generated *via* the two paradigms decreased as constant-rate stimulus increased. (D) The difference between hysteretic forces and constant-rate only forces is quantified as in Fig. 4, such that a doubling of force is quantified as a 100% increase. Hysteretic force gains diminish with constant-rate stimulus frequency (% increase=49.80e$^{-0.087}$, $R^2$=0.91, $N$=59). Only positive error bars are plotted.
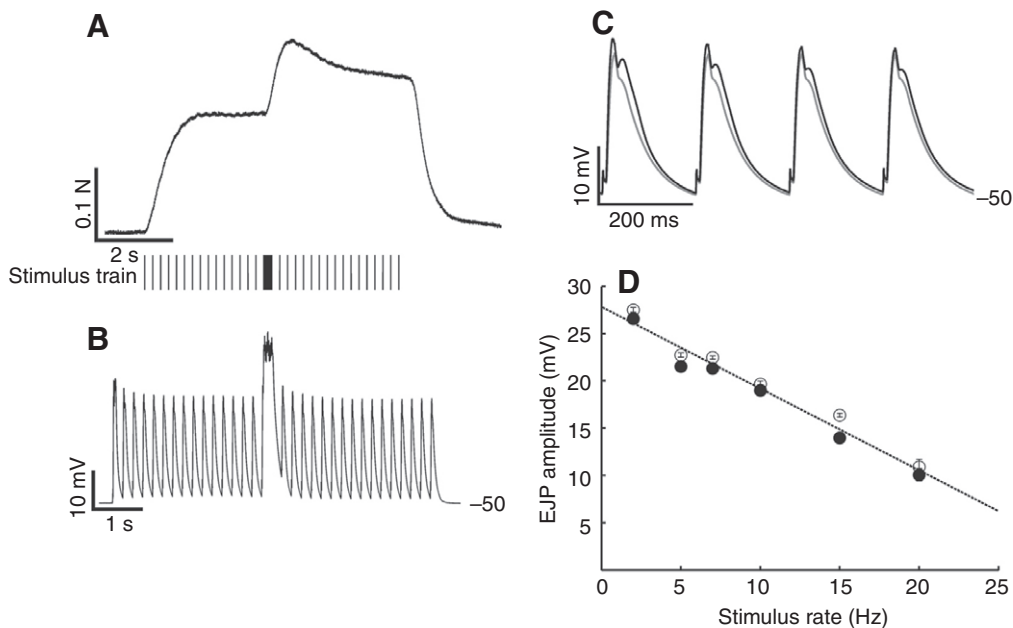


Fig. 6. Muscle voltage is not different before and after hysteretic bursts of stimuli. (A) An example force recording from the semi-intact preparation is shown with the stimulus train indicated below. (B) Excitatory junction potentials (EJPs) are recorded from one of the longitudinal M6 muscles during the stimulus paradigm shown in panel A. (C) Signal means of EJPs from constant-rate stimulus trains before (black) and after (gray) a hysteretic burst. The signal means are synchronized to the second stimulus after either the beginning of the experiment or after a hysteretic burst ($N$=35 records, each). (D) The mean amplitude of EJPs at various stimulation rates is plotted before a hysteretic burst (open circles) and after the burst (filled circles) ($N$=20 animals, 400 trials). Generally, as constant-rate stimulation frequency increases, EJP amplitude decreases linearly. EJP–rate curves were both well fit by one line: EJP=−0.86(rate)+27.83 [$R^2_{semi-intact}$=0.95 and $R^2_{single}$=0.96, $P$<<0.01, both Pitman's Normal Correlation (Pitman, 1939)]. However, successive EJPs within a single train of stimulation remain relatively unchanged (error bars are s.e.m.).
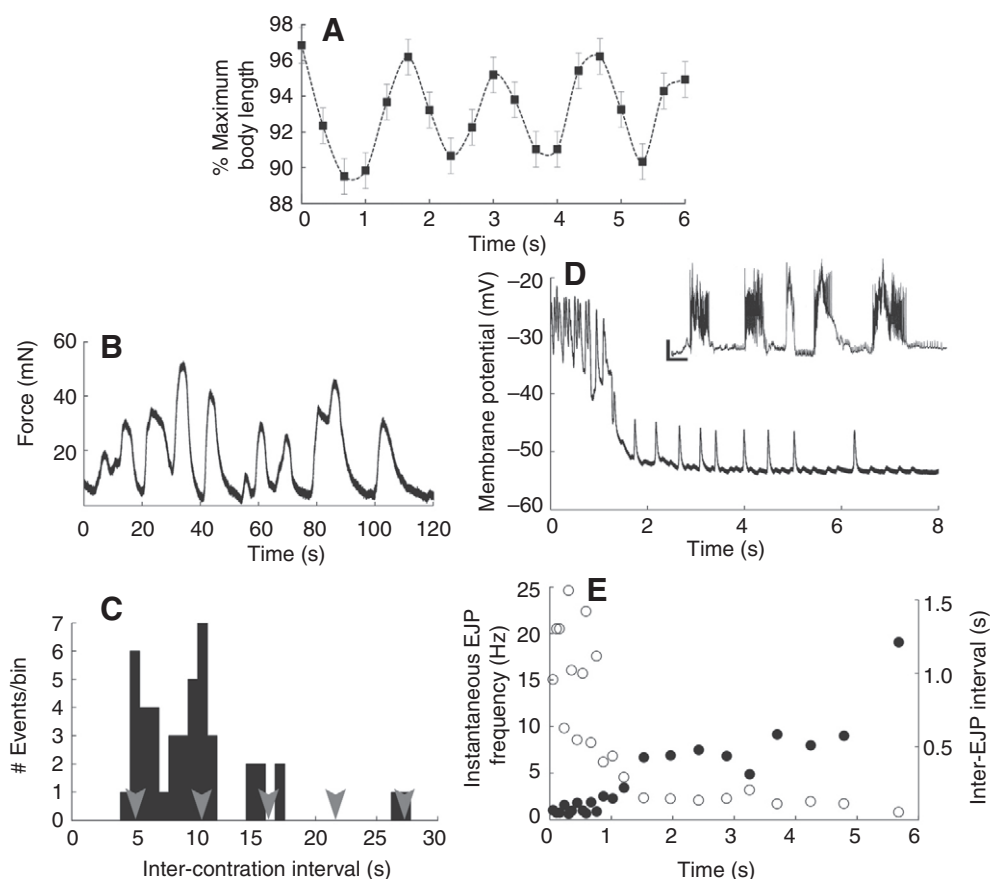
Fig. 7. Kinematics and physiological parameters of undulatory contraction. (A) Body length of intact animals cycles over time with a mean period of ~0.83 Hz. Body length is plotted as a percentage of maximum observed length during locomotion videos (*N*=8). (B) Semi-intact preparations rhythmically contract with a frequency of about 5.5 Hz (typical example shown, *N*=4 animals, 45 contractions). (C) A histogram of inter-contraction intervals (semi-intact) illustrates the periodicity of contractions (gray arrowheads are at 5.5 s intervals). (D) An example of excitatory junction potentials (EJPs) that underlay a spontaneous contraction, recorded from a central segment (M6, segment 4). Inset a longer period is plotted for comparison with the contraction rate in panel (B), scale bar: 5 mV, 2 s. (E) The rate of EJPs decays rapidly from ~25 Hz to ~1 Hz upon termination of the contraction (open circles), rates were computed from the inter-EJP interval (closed circles) shown above.

stimulus frequency during both the rising and falling phase (Fig. 8C). We also modulated frequency between 2 Hz and 25 Hz over a slightly longer period (~10 s, Fig. 8D). Under these conditions, positive hysteresis persisted but at a lesser magnitude which decayed more after each cycle than when modulating across lower rates (Fig. 8E). This successive reduction in hysteresis (Fig. 8F) is a product of not only lesser differences in force between rising and falling phases within individual cycles (greatest peak force; Fig. 8C=0.48 N, Fig. 8F=0.38 N), but also a greater reduction from cycle to cycle (range of peak force across cycles: Fig. 8C=0.16 N; Fig. 8F=0.24 N).

## DISCUSSION

Wandering stage third instar *Sarcophaga bullata* and *Drosophila melanogaster* larvae have the capacity for hysteretic force production. Physiological and behavioral parameters of neuromuscular activation (Fig. 7) correspond to the range wherein hysteretic force increases are significant, across relatively low frequency values. Although peak EJP frequency approached 25 Hz during rhythmic activation by the intact nervous system, the larval muscle most often received much slower rates of synaptic activation. During modulated frequency stimulation, animals exhibited positive hysteresis.

We recorded synaptic potentials from body wall muscles during hysteretic contractions and found neither facilitation nor long-term potentiation, once putative explanations for the increased force production. This does not eliminate subtle changes in voltage from the cascade of signals which may be involved in hysteresis. To test that hypothesis, it may be useful to challenge synaptic transmission at the neuromuscular junction with reduced calcium or with a mutant of muscle glutamate receptors. Despite a healthy safety factor at the larval neuromuscular junction (Marrus and DiAntonio, 2005), we expect that modification of EJP amplitude will inform our understanding of hysteretic mechanisms. Specifically, if positive hysteresis is not proportional to changes in synaptic transmission, its activation may involve shortening or strain rather than voltage. Additionally, it is possible that higher rate activation of motoneurons may modify the migration of dense core vesicles, as indicated by studies delivering considerably more stimuli to the segmental nerves (Shakiryanova et al., 2007).

The value of positive force hysteresis to larval crawling behavior remains an interesting question. Although some reduction in energy expenditure is putatively gained, it remains unclear why an organism with simple rhythmic motor behavior would utilize a dynamic property of contraction (i.e. doubling force production at a given motoneuron rate). As gain in the motoneuron rate–muscle force relationship changes, a given efferent signal – designed upstream in the central nervous system
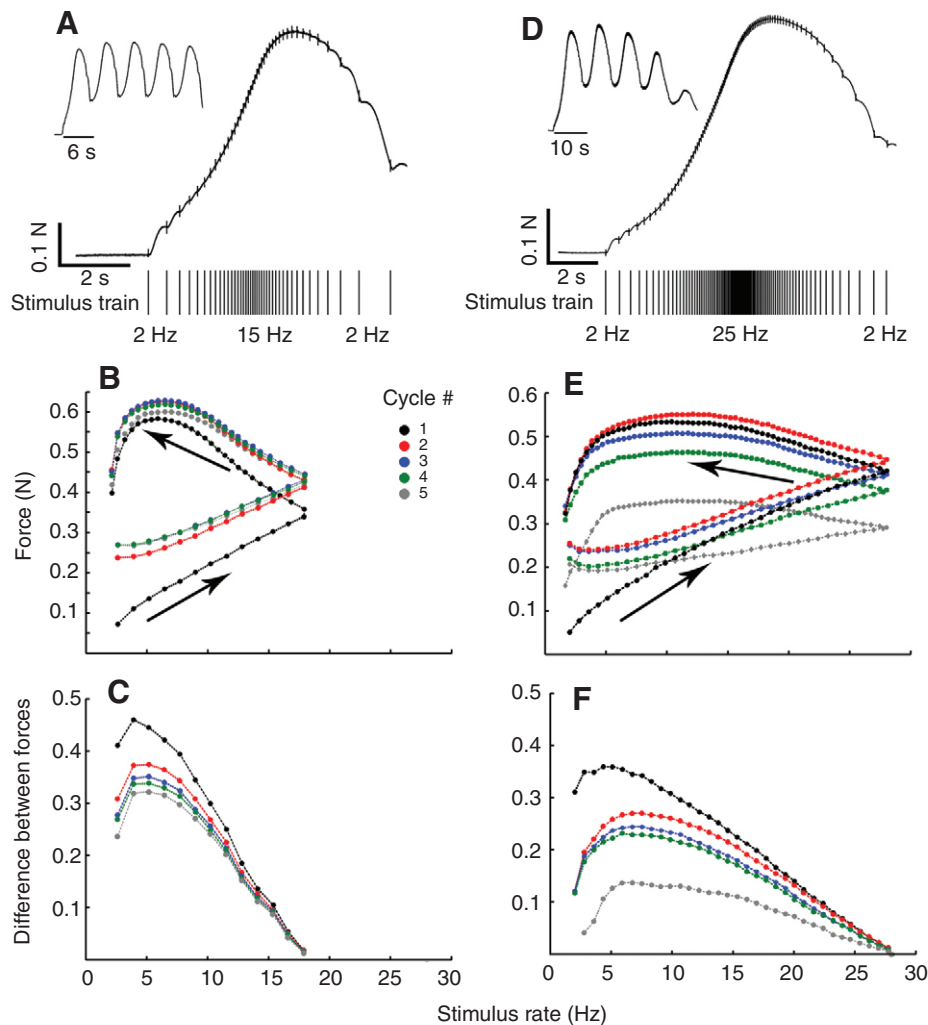
Fig. 8. Force produced by frequency modulation of stimulus frequency (*Sarcophaga*). (A) Cyclical stimulation from 2 Hz to 15 Hz over a cycle period of ~6 s of semi-intact preparations yields non-symmetrical force contractions (*N*=9 animals, 36 cycling routines). The stimulus train used for these trials is shown beneath the force traces. (B) Frequency-modulated loops illustrate the difference in force generated at equal stimulus frequencies but as contraction cycles rise and fall. Force increases with stimulus rate (rightward arrows) during the initial contraction phase but as stimulus rate peaks and begins its decent, force continues to grow before more slowly decaying (leftward arrow). (C) The difference between forces generated by increasing stimulus rate and those upon decreasing rate are plotted per stimulation frequency. Each successive contraction is plotted in a different color (cycles 1–5 are indicated by black, red, blue, green and gray, respectively). (D–F) Same as left columnar panels but based on data shown in B, which modulates between 2 Hz and 25 Hz over a cycle period of 10 s.

– will yield varied output. As mentioned earlier and in previous work (Zill and Jepson-Innes, 1988), this form of motor plasticity thus presents a dynamic control problem to the nervous system. One means of mediating the computational demand of that problem would be to utilize a gain sensor in the periphery and feed it into the Central Pattern Generator (CPG) responsible for undulatory locomotion. The chordotonal organs of larval *Drosophila* do indeed appear to feed into the CPG of the central nervous system (Caldwell et al., 2003), although there is no evidence that these stretch receptors transduce gain in the rate–force relationship. We know of no other receptors in the larvae that are in a position to relay gain and thus are left with the control problem presented by dynamic changes in the rate–force relationship.

We have made detailed comparison of forces recorded from semi-intact and single-muscle preparations to establish the former as a reasonable estimate (in sum) of the latter. The proportionality of single muscle force records with semi-intact records speaks to several points: that tissue at the origin or insertion is not likely to play a central role in the production of hysteretic forces. Because the exponential functions describing hysteretic gains in the rate–force curve from single muscle, semi-intact and the smaller *Drosophila* preparations were similar (*Sarcophaga*, Fig. 4E,F; *Drosophila*, Fig. 5D), we find no reason to suggest the various connective tissues contribute to the phenomenon. However, the differences between data of semi-intact (Fig. 4C) and single muscle preparations (Fig. 4D) deserve closer examination in future experiments. The hysteretic and constant-rate curves acquired from single muscle preparations appeared more linear than comparable data from semi-intact preparations but the residuals of the exponential fit for data computed from single muscle did not favor a linear fit equation. The linearity of the rate–force relationship acquired from single muscle experiments may indicate a contribution from a non-contractile, elastic element that persisted upon ablation of the

surrounding segments and musculature. Tissues or proteins capable of storing elastic energy might offset force gains at the highest growth phase of the rate–force curve (e.g. kettin and titin) (Hooper and Thuma, 2005). In this scenario, however, candidate energy-storage molecules would need a time-constant of sufficient duration (e.g. ~1 s) to mask transient force gains.

The proportionality of single muscle recordings to semi-intact also points to which muscle groups are involved in longitudinal contraction. It appears that the four main longitudinal muscles (ventrally: M6, 7, 12 and 13) are the primary longitudinal contractors during length change, and that transverse musculature does not contribute notably to longitudinal force recordings. During semi-intact experiments, we gathered all segmental nerves (severed) for stimulation. The musculature of the terminal (i.e. conical) segments was immobilized *via* gluing to the tabs used in recording force, leaving eight freely contracting segments (*Sarcophaga*; 12 segments), each of which is highly stereotyped (Keshishian et al., 1996; Feeney et al., 1998). The ratio of force values obtained from semi-intact preparations to those from single muscle recordings was 55.14 (±3.84):1. This is close to the predicted ratio, 64, which represents four ventral longitudinal muscles, per side, per segment. The observed ratio is satisfactory because in *Sarcophaga* the anterior segments A3–A4 are approximately one-third smaller in diameter than A5–A10, thus putatively contributing less force. Moreover, intracellular recording from the largest longitudinal fiber (M6) may have impeded contraction in those few fibers from which recordings were made. Taken together, these observations suggest a prediction of marginally less than 64:1. Estimating 2/3 force contribution from terminal segments (relative to central segments) yields a ratio of 58.56:1.

Lastly, the observed ratio between single and semi-intact forces suggests that transverse muscles contribute only small amounts, if at all, to longitudinal shortening. The ventral transverse muscles are nevertheless positioned – on average ~30 deg off the longitudinal centerline – to contribute to the longitudinal force vector and are innervated by the segmental nerves we stimulated (Keshishian et al., 1996). Although we cannot exclude their contribution, additional contribution by these muscles would raise the predicted force ratio substantially (~78:1; six ventral transverse muscles per segment, ~30 deg off longitudinal centerline, eight segments).

We did not report force generation by single muscles or single segments of *Drosophila* larvae because the magnitude of those data was too close to the amplitude of noise. Means of force traces obtained over many trials at lower-frequency stimulation (i.e. <10 Hz) produced results but these were not of satisfactory quality nor were they crucial to our investigation of the questions addresses herein.

A phenomenon that was prevalent in frequency-modulated activation of the muscles was the gradual reduction in force magnitude over the duration of experiments. Typically, we gathered data during the initial 40–50 min post-dissection, and although forces could be obtained later, they continued to decay in magnitude until the muscle failed to produce force upon stimulation. We terminated experiments upon first recognition of such run-down and utilized the above described normalization procedure (see Materials and methods) to account for any progressive changes, albeit small, in contractile elements during experimentation. We believe this normalization successfully attenuated time-dependent changes in contractibility, also noted by others (Wanischeck and Rose, 2006), as our recordings are in good agreement with other reports of isometric contraction. Interestingly, synaptic potentials persisted long after contractions faded and did not exhibit signs of decay. It is possible that our *Sarcophaga* saline, an insect Ringer's solution

referenced by Strausfeld et al. (Strausfeld et al., 1983), may benefit from customization to the larval body wall tissue as HL-3 was customized for *Drosophila* by Stewart et al. (Stewart et al., 1994).

The molecular mechanism(s) of hysteretic force gains are not understood. Although much is known about a few specialized systems, such as mulluscan catch tension (Andruchov et al., 2006), even these systems leave much to be explored. For example, it is known that both pH and cAMP profoundly modulate tension in mulluscan catch fibers but the precise site of this action and the molecular changes it elicits are not yet clear (Avrova et al., 2009). Recent work in *Drosophila* indicates that force is modulated by several peptides (Hewes et al., 1998; Clark et al., 2008) as well as the biogenic amines tyramine and octopamine (Wanischeck and Rose, 2006). Those results, and the possibility of links to mulluscan catch fibers, provide clear paths for future investigations in a model system such as the larval *Diptera* described here.

We utilized isometric recordings, which are among the first to be reported from *Drosophila*. During the preparation of this manuscript, one other group has communicated isometric force recordings in *D. melanogaster* (Rose et al., 2007; Wanischeck and Rose, 2006). Although these studies examined contractions of single segments of *Drosophila* larvae using a slightly different transducer configuration, the magnitude and timescale of forces they report are in good agreement with ours. Isometric recordings provide favorable qualities for quantitative examination of muscle dynamics, including improved control of muscle and sarcomere length (and thus consistency along the length–tension curve) to better compare animals of varied size, and superior resolution which is less confounded by transducer mechanics. Together with isotonic force recordings (Hewes et al,. 1998; Clark et al., 2008), advances in muscle recording from Dipteran larvae stand to illuminate links between molecular phenomenon and behavior.

Muscle plasticity is of increasing interest across a broad diversity of organisms [Arthropoda (Zill et al., 1992; Woods et al., 2008); Chordata (Herzog and Leonard, 2002; Harrison et al., 2008); Mullusca (Andruchov et al., 2006; Avrova et al., 2009)] with applications spanning biology and engineering (Dorfmann et al., 2008; Lin et al., 2009). We are excited by the prospect of investigating this form of post-synaptic plasticity using the extraordinary tools available with larval Dipteran preparations.

## LIST OF ABBREVIATIONS

| | |
|---|---|
| CPG | Central Pattern Generator |
| $d$V | voltage difference |
| EJP | excitatory junction potential |
| M6, 7, 12 and 13 | longitudinal body wall muscles # 6, 7, 12 and 13 |
| $V_m$ | membrane potential |

## REFERENCES

**Abbott, B. C. and Aubert, X. M.** (1952). The force exerted by active striated muscle during and after change of length. *J. Physiol.* **117**, 77-86.

**Allen, W., Charlton, M. and Montgomery, A.** (1980). Semiconductor force transducer suitable for use with small muscles. *Med. Biol. Eng. Comput.* **18**, 378-380.

**Andruchov, O., Andruchova, O. and Galler, S.** (2006). The catch state of mullusc catch muscle is established during activation: experiments on skinned fiber

preparations of the anterior byssus retractor muscle of *Mytilus edulis* L. using the myosin inhibitors orthovanadate and blebbistatin. *J. Exp. Biol.* **209**, 4319-4328.

**Avrova, S. V., Shelud'ko, N. S., Borovikov, Y. S. and Galler, S.** (2009). Twitchin of mollusc smooth muscles can induce 'catch'-like properties in human skeletal muscle: support for the assumption that the 'catch' state involves twitchin linkages between myofilaments. *J. Comp. Physiol. B.* **179**, 945-950.

**Berrigan, D. and Lighton, J. R. B.** (1993). Bioenergetic and kinematic consequences of limblessness in larval *Diptera. J. Exp. Biol.* **179**, 245-259.

**Berrigan, D. and Pepin, D. J.** (1995). How maggots move: allometry and kinematics of crawling in larval *Diptera. J. Insect Physiol.* **41**, 329-337.

**Blaschko, H., Cattell, M. and Kahn, J. L.** (1931). On the nature of the two types of response in the neuromuscular system of the crustacean claw. *J. Physiol.* **73**, 25-35.

**Burke, R. E., Rudomin, P. and Zajac, F. E., III** (1970). Catch property in single mammalian motor units. *Science* **168**, 122-124.

**Caldwell, J. C., Miller, M. M., Wing, S., Soll, D. R. and Eberl, D. F.** (2003). Dynamic analysis of larval locomotion in *Drosophila* chordotonal organ mutants. *Proc. Natl. Acad. Sci. USA* **100**, 16053-16058.

**Clark, J., Milakovic, M., Cull, A., Klose, M. K. and Mercier, A. J.** (2008). Evidence for postsynaptic modulation of muscle contraction by a *Drosophila* neuropeptide. *Peptides* **29**, 1140-1149.

**David, J. R.** (1962). A new medium for rearing *Drosophila* in axenic condition. *Drosophila Inf. Serv.* **36**, 128.

**Donaldson, I. M. L. and Knox, P. C.** (2000). Afferent signals from the extraocular muscles affect the gain of the horizontal vestibule-ocular reflex in the alert pigeon. *Vis. Res.* **40**, 1001-1011.

**Dorfmann, L., Woods, W. A., Jr and Trimmer, B. A.** (2008). Muscle performance in a soft-bodied terrestrial crawler: constitutive modeling of strain-rate dependency. *J. R. Soc. Interface* **5**, 349-362.

**Eccles, J. C., Katz, B. and Kuffler, S. W.** (1941). Nature of the 'endplate potential' in curarized muscle. *J. Neurophysiol.* **4**, 362-387.

**Feeney, C. J., Karunanithi, S., Pearce, J., Govind, C. K. and Atwood, H. L.** (1998). Motor nerve terminals on abdominal muscles in larval flesh flies, *Sarcophaga bullata*: comparisons with *Drosophila. J. Comp. Neurol.* **402**, 197-209.

**Fox, L. E., Soll, D. R. and Wu, C.-F.** (2006). Coordination and modulation of locomotion pattern generators in *Drosophila* larvae: effects of altered biogenic amine levels by the tyramine β hydroxlyase mutation. *J. Neurosci.* **26**, 1486-1498.

**Griffith, L. C. and Budnik, V.** (2006). Plasticity and second messengers during synapse development. *Int. Rev. Neurobiol.* **75**, 237-265.

**Harrison, S. M., Lamont, C. and Miller, D. J.** (2008). Hysteresis and the length dependence of calcium sensitivity in chemically skinned rat cardiac muscle. *J. Physiol.* **401**, 115-143.

**Herzog, W. and Leonard, T. R.** (2002). Force enhancement following stretching of skeletal muscle: a new mechanism. *J. Exp. Biol.* **205**, 1275-1283.

**Hewes, R. S., Snowdeal, E. C., 3rd, Saitoe, M. and Taghert, P. H.** (1998). Functional redundancy of FMRFamide-related peptides at the *Drosophila* larval neuromuscular junction. *J. Neurosci.* **18**, 7138-7151.

**Hooper, S. and Thuma, J.** (2005). Invertebrate muscles: muscle specific genes and proteins. *Physiol. Rev.* **85**, 1001-1060.

**Hoyle, G.** (1983). *Muscles and Their Neural Control*, 689 pp. New York: John Wiley and Sons.

**Hunt, C. C.** (1990). Mammalian muscle spindle: peripheral mechanisms. *Physiol. Rev.* **70**, 643-663.

**Keshishian, H., Broadie, K., Chiba, A. and Bate, M.** (1996). The *Drosophila* neuromuscular junction: a model system for studying synaptic development and function. *Annu. Rev. Neurosci.* **19**, 545-575.

**Krans, J. L. and Chapple, W. D.** (2005). Variability of motoneuron activation and the modulation of force production in a postural reflex of the hermit crab abdomen. *J. Comp. Physiol. A* **191**, 761-775.

**Krans, J. L., Rivlin, P. K. and Hoy, R. R.** (2005). Demonstrating the temperature sensitivity of synaptic transmission in a *Drosophila* mutant. *J. Undergrad. Neurosci.* **4**, A27-A33.

**Krans, J. L., Parfitt, K. D., Rivling, P. K., Gawera, K. D. and Hoy, R. R.** (2010). The resting membrane potential of *Drosophila melanogaster* larval muscle depends strongly on external calcium concentration. *J. Insect Physiol.* **56**, 304-313.

**Lappin, A. K., Monroy, J. A., Pilarski, J. Q., Zepnewski, E. D., Pierotti, D. J. and Nishikawa, K. C.** (2006). Storage and recovery of elastic potential energy powers ballistic prey capture in toads. *J. Exp. Biol.* **209**, 2535-2553.

**Lin, H.-T., Dorfmann, A. L. and Trimmer, B. A.** (2009). Soft-cuticle biomechanics: a constitutive model of anisotropy for caterpillar integument. *J. Theor. Biol.* **256**, 447-457.

**Marder, E. and Bucher, D.** (2007). Understanding circuit dynamics using the stomatogastric nervous system of lobsters and crabs. *Annu. Rev. Physiol.* **69**, 291-316.

**Marrus, S. B. and DiAntonio, A.** (2005). Investigating the safety factor at an invertebrate neuromuscular junction. *J. Neurobiol.* **63**, 62-69.

**Nadim, F., Manor, Y., Kopell, N. and Marder, E.** (1999). Synaptic depression creates a switch that controls the frequency of an oscillatory circuit. *Proc. Natl. Acad. Sci. USA* **96**, 8206-8211.

**Nivens, J. E. and Burrows, M.** (2003). Spike width reduction modifies the dynamis of short-term depression at a central synapse in the locust. *J. Neurosci.* **23**, 7461-7469.

**Pan, B. and Zucker, R. S.** (2009). A general model of synaptic transmission and short-term plasticity. *Neuron* **62**, 539-554.

**Paterson, B. A. and Krans, J. L.** (2009). Hysteresis in force production of bodywall muscle of larval *Diptera. Society for Integrative and Comparative Biology [SICB] Annual Meeting*, Boston, MA. Final Program and Abstracts P2.147, p. 85.

**Pette, D. and Vrbová, G.** (1999). What does chronic electrical stimulation teach us about muscle plasticity. *Muscle Nerve* **22**, 666-677.

**Pitman, E. G.** (1939). A note on normal correlation. *Biometrika* **31**, 9-12.

**Rose, U., Derst, C., Wanischeck, M., Marinc, C. and Walther, C.** (2007). Properties and possible function of a hyperpolarisation-activated chloride current in *Drosophila. J. Exp. Biol.* **210**, 2489-2500.

**Shakiryanova, D., Klose, M. K., Zhou, Y., Gu, T., Deitcher, D. L., Atwood, H. L., Hewes, R. S. and Levitan, E. S.** (2007). Presynaptic ryanodine receptor-activated calmodulin kinase II increases vesicle mobility and potentiates neuropeptide release. *J. Neurosci.* **27**, 7799-7806.

**Stewart, B. A., Atwood, H. L., Renger, J. J., Wang, J. and Wu, C.-F.** (1994). Improved stability of *Drosophila* larval neuromuscular preparations in haemolymph-like physiological solutions. *J. Comp. Physiol. A* **175**, 179-191.

**Strausfeld, N., Seyan, H. S., Wohlers, D. and Bacon, J. P.** (1983). Lucifer yellow histology. In *Functional Neuroanatomy* (ed. N. Strausfeld), pp. 132-155. Berlin: Springer Publishing.

**Twarog, B. M.** (1972). Aspects of smooth muscle function in mulluscan catch muscle. *Physiol. Rev.* **56**, 829-838.

**Wanischeck, M. and Rose, U.** (2006). Contraction measurements in body wall muscles of *Drosophila* larvae reveal modulatory effects of octopamine and its precursor tyramine. *Society for Neuroscience Annual Meeting,* Atlanta, GA. Final Program and Abstracts 592.8.

**Wilson, D. M. and Larimer, J. L.** (1968). The catch property of ordinary muscle. *Proc. Natl. Acad. Sci. USA* **61**, 909-916.

**Wilson, D. M., Smith, D. O. and Dempster, P.** (1970). Length and tension hysteresis during sinusoidal and step function stimulation of arthropod muscle. *Am. J. Physiol.* **218**, 916-922.

**Woods, W. A., Jr, Fusillo, S. J. and Trimmer, B. A.** (2008). Dynamic properties of a locomotory muscle of the tobacco hornworm *Manduca sexta* during strain cycling and simulated natural crawling. *J. Exp. Biol.* **211**, 873-882.

**Zill, S. N. and Jepson-Innes, K.** (1988). Evolutionary adaptation of a reflex system: sensory hysteresis counters muscle 'catch' tension. *J. Comp. Physiol. A* **164**, 43-48.

**Zill, S. N., Frazier, S. F., Lankenau, J. and Jepson-Innes, K.** (1992). Characteristics of dynamic postural reactions in the locust hindleg. *J. Comp. Physiol. A* **170**, 761-772.